PHYSICAL REVIEW B **87**, 024107 (2013)

Domain formation and dielectric response in $PbTiO_3$: A first-principles free-energy landscape analysis

Anil Kumar,[1,2] Karin M. Rabe,[1] and Umesh V. Waghmare[2]
[1]*Department of Physics and Astronomy, Rutgers University, Rutgers, New Jersey 08854 USA*
[2]*Theoretical Sciences Unit, Jawaharlal Nehru Centre for Advanced Scientific Research, Bangalore 560064, India*
(Received 17 August 2012; published 22 January 2013)

We determine the relative thermodynamic stability of competing homogeneously and inhomogeneously ordered ferroelectric phases of $PbTiO_3$ using its free-energy landscape, obtained from constrained-polarization molecular-dynamics simulations with a first-principles effective Hamiltonian and thermodynamic integration. While we find that the tetragonal structure is thermodynamically most stable at temperatures below the ferroelectric transition temperature ($T_0 = 660$ K), the free energy of an "orthorhombic-like" 90° domain phase relative to the tetragonal phase almost vanishes at $T = 540$ K and remains small at all temperatures below T_0. In contrast to $BaTiO_3$, the 90° domain structure is an order of magnitude lower in energy than the one with 180° domains. We show that the dielectric response contains signatures of such a domain structure and is significantly stronger than that of the uniformly polarized tetragonal phase of $PbTiO_3$.

DOI: 10.1103/PhysRevB.87.024107 PACS number(s): 77.80.Dj, 77.80.B−

I. INTRODUCTION

A ferroelectric is a material with a polar phase produced by a structural transition from a nonpolar high-symmetry paraelectric state, with an electric polarization that can be switched between two or more symmetry-related variants by application of an electric field.[1] The characteristic behavior of ferroelectrics in applied electric fields gives rise to many important technological applications, including nonvolatile ferroelectric random-access memories, piezoelectric sensors and actuators, microelectromechanical systems, and high-dielectric-constant materials for electronics.[2–5]

When a ferroelectric material is cooled below its transition temperature in the absence of an external electric field, it typically forms complex microstructures consisting of many small regions with different orientations of the spontaneous polarization known as domains. Such domains form spontaneously to reduce the uncompensated depolarization field at the surface of the crystal and hence to reduce the free energy of the system.[1] A precise understanding of the microstructure of these ferroelectric domains and their dynamics as a function of external conditions such as temperature, pressure, and electric field is highly desirable for applications in devices. For example, knowledge of the width of domain walls, nucleation of domains, and their growth is directly relevant to how fast polarization can be switched and hence to applications in memory devices.[2]

Landau-Ginzburg phenomenological free-energy functionals have long proved very useful in describing the behavior of ferroelectrics[6–9] relevant to modeling and simulations of ferroelectric-based devices. From the knowledge of the free-energy landscape one can determine various stable and metastable states as well as minimum-energy pathways of transition between them. For example, one can understand switching of polarization from one equilibrium state to another, relevant to applications of a ferroelectric in memory devices. The functionals can include terms to describe domain walls and can be used in studies of domains and other inhomogeneously ordered states of ferroelectrics.[10,11] However, they are limited by the fact that the parameters in the functional are determined phenomenologically, and the connection to the microscopic energetics is not clear.

First-principles calculations have been quite effective in accessing microscopic information about the structural energetics of ferroelectric materials[12,13] and even predicting phase-transition behavior at finite temperature through construction of effective Hamiltonians.[14–18] Recently, a method was developed to obtain free energies and a Landau-Ginzburg type of continuum theory[19–21] of ferroelectrics starting from a first-principles effective Hamiltonian.[22–25] This construction bridges the gap between first-principles results and the Landau approach to describe behavior at longer length scales; it provides a predictive method for determining parameters and extending the form of the functional to include additional terms and gives insight into the microscopic origin of the features of the free-energy landscape. $PbTiO_3$ is one of the most studied ferroelectric materials both experimentally and from first-principles calculations. It has a transition at ≈760 K from the high-temperature cubic perovskite paraelectric phase (space group $Pm\bar{3}m$, # 221) to a low-temperature tetragonal ferroelectric phase (space group $P4mm$, number 99) with a large electric polarization (≈75 $\mu C/cm^2$).

In this paper, we perform first-principles constrained-polarization molecular-dynamics (MD) simulations for $PbTiO_3$ and determine the free-energy landscape as a function of polarization for a range of temperatures to find the relative stability of different phases and determine parameters in a Landau functional that describes uniform configurations of $PbTiO_3$ near T_c. We also study the free-energy landscape for inhomogeneously ordered configurations of polarization using an augmented form of the effective Hamiltonian that provides information about the energetics of formation of domains and domain-wall energy. For these inhomogeneous configurations, calculation of the dielectric response due to phonons and fluctuations of domain walls shows significant enhancement relative to the configurations without domain walls, even in the absence of contributions from uniform domain-wall motion, which are not accessible on the time scales of the simulations. We discuss the relevance to experimental observations.

TABLE I. The values of the parameters of the first-principles effective Hamiltonian for $PbTiO_3$ used in our simulations. The third column shows how these parameters are determined from the parameters given in Ref. 17.

Parameters	Value	Relation
a_0 (Å)	3.969	a_0
B_{11} (eV)	117.9	C_{11}
B_{12} (eV)	51.6	C_{12}
B_{44} (eV)	137.0	C_{44}
B_{1xx} (eV/Å^2)	−114.02	$2(g_0+g_1)$
B_{1yy} (eV/Å^2)	−13.67	$2g_0$
B_{4yz} (eV/Å^2)	−22.67	g_2
α (eV/Å^4)	27.83	$B+C$
γ (eV/Å^4)	−34.48	$-2C$
k_1 (eV/Å^6)	−42.42	D
k_2 (eV/Å^6)	0	
k_3 (eV/Å^6)	0	
k_4 (eV/Å^8)	156.43	E
m^* (amu)	100.0	
Z^* (e)	10.02	Z^*
ϵ_∞	8.24	ϵ_∞
κ_2(eV/Å^2)	1.170	A
j_1 (eV/Å^2)	−1.355	$2a_T$
j_2 (eV/Å^2)	4.986	$2a_L$
j_3 (eV/Å^2)	0.222	b_l+b_{t1}
j_4 (eV/Å^2)	−0.018	$2b_{t2}$
j_5 (eV/Å^2)	0.398	b_l-b_{t1}
j_6 (eV/Å^2)	−0.083	$\frac{2(c_l+2c_t)}{3}$
j_7 (eV/Å^2)	−0.204	$\frac{2(c_l-2c_t)}{3}$

II. COMPUTATIONAL METHODS

A. Effective Hamiltonian

A first-principles effective Hamiltonian is a parametrization of the energy surface in the subspace of important degrees of freedom, with parameters obtained from first-principles density functional theory total-energy calculations.[13–17] A first-principles effective Hamiltonian for $PbTiO_3$, in terms of local dipolar distortions and strain, has been previously constructed;[17] we use this effective Hamiltonian in the present work. In order to perform the simulations with the FERAM code, described in more detail below, we transformed it into the equivalent form given in Refs. 18, 26, and 27. In Table I, we give the values of the parameters in this latter form and show how they are determined from the parameters given in Ref. 17. The sixth-order anisotropy terms (k_2 and k_3) are not present in the effective Hamiltonian of Ref. 17 and are set to zero in the present calculations.

B. MD simulations of bulk $PbTiO_3$

We performed molecular-dynamics simulations using the first-principles effective Hamiltonian specified in the previous section. We used the mixed-space molecular-dynamics code FERAM,[26–28] in which the long-range interactions are treated in reciprocal space[29,30] to perform both heating-up and cooling-down simulations in a simulation box of $L_x \times L_y \times L_z$ unit cells with periodic boundary conditions. A Nose-Poincaré thermostat[31] is used to maintain constant temperature, which allows us to use a relatively large time step of 2 fs. In the cooling-down simulations, we started with a random configuration of local dipoles at high temperature ($T \geqslant T_c$, 900 K), performed a thermalization run of 100 000 time steps, and then performed an averaging run of 100 000 time steps. The temperature was then decreased by 10 K, and the thermalization and averaging processes were repeated using the final configuration from the previous temperature as an initial configuration for the new temperature. In the heating-up simulations, we started with uniformly aligned local dipoles along the z direction at low temperature ($T = 200$ K), performed a thermalization run of 100 000 time steps, and then performed an averaging run of 100 000 time steps. The temperature was then increased by 10 K, and the thermalization and averaging processes were repeated as in the cooling-down simulations.

The polarization of a system is given by $\vec{P} = \frac{Z^* \sum_i \vec{\xi}_i}{\Omega}$, where $\vec{\xi}_i$ is the local mode at each site, Z^* is the mode effective charge, and Ω is the total volume of the system. The sum over i runs over all unit cells in the system. The dielectric constant of the system is determined from the fluctuations in polarization.

$$\epsilon = \frac{\Omega[\langle \vec{P}^2 \rangle - \langle \vec{P} \rangle^2]}{\epsilon_0 k_B T}, \tag{1}$$

where k_B is the Boltzmann constant and T is temperature.

C. Simulations with constrained polarization and domains

To obtain the value of the Ginzburg-Landau free-energy function for a given macroscopic polarization and temperature, we used a thermodynamic integration method with the results of constrained-polarization molecular-dynamics simulations. This procedure is the one used in our previous work on $BaTiO_3$ (Ref. 23) and is analogous to that used by Geneste.[25] To constrain polarization to a given value in the simulation, we augmented the first-principles effective Hamiltonian H_0 of $PbTiO_3$ with three terms. This yields

$$H = H_0 - Z^* \vec{E} \cdot \sum_i \vec{\xi}_i + \Omega \vec{P} \cdot \vec{E} - \frac{\Omega}{8\pi} \sum_{\alpha\beta} \left(\epsilon^\infty_{\alpha\beta} - \delta_{\alpha\beta}\right) E_\alpha E_\beta, \tag{2}$$

where $\vec{P}$ is the target polarization, i is an index for the lattice sites, $\vec{\xi}_i$ is the local polar distortion vector[32] describing the displacements of atoms near site i, and $\vec{E}$ is an auxiliary fluctuating electric field to keep the average polarization of the system at the target value. The modified Hamiltonian H [Eq. (2)] ensures that sampling in molecular-dynamics simulations will yield the target average polarization.

Once we have the auxiliary electric field $\langle E(P) \rangle$ for a range of polarization at a given temperature, we can use the thermodynamic integration method[33] to determine the free energy as a function of polarization and temperature. For a given temperature, the free-energy difference between two polarization states P_1 and P_2 is given as

$$\Delta F_H = \int_{\vec{P}_1}^{\vec{P}_2} \langle \vec{E}(\vec{P}') \rangle d\vec{P}'. \tag{3}$$

We point out that constraining the total polarization of the system to a value smaller than its equilibrium value can

result in a configuration with domains, as has been observed in earlier works[23,25] on $BaTiO_3$. This is observed for large system sizes because the gain in energy due to changing the polarization to its equilibrium value within a domain scales with the volume of the domain, while the energy cost of domain walls needed to create the domain scales with surface area. The formation of an inhomogeneous configuration as a result of constraint on the order parameter to a value smaller than its equilibrium value is a very general phenomenon and has been observed in other systems.[22,34] The free energy of such inhomogeneously ordered configurations can be represented in a Ginzburg-Landau theory by adding terms that depend on divergence and curl of the order parameter.[23]

With a generalized form of the augmented first-principles effective Hamiltonian, we can impose a constraint on the spatially varying polarization, where $\vec{E}^D$ is an auxiliary fluctuating electric field that is allowed to take different values on different lattice sites. This allows us, for example, to study a system with a domain wall.

$$H = H_0 - Z^* \vec{E}^D \cdot \sum_i \xi_i \hat{e}_i + \Omega \vec{P}^D \cdot \vec{E}^D - \frac{\Omega}{8\pi} \sum_{\alpha\beta} \left(\epsilon^{\infty}_{\alpha\beta} - \delta_{\alpha\beta}\right) E^D_\alpha E^D_\beta, \quad (4)$$

where a superscript D means domain (or it can be a configuration characterized by spatially dependent polarization), $\hat{e}_i$ is the unit vector along the direction of this configuration in the phase space, and $\vec{E}^D$ is the analog of $\vec{E}$ for domain configurations. To access a configuration consisting of domains of two opposite orientations, we set $\hat{e}_i = (111)$ for sites i in the first domain and $\hat{e}_i = (\bar{1}\bar{1}\bar{1})$ for sites i in the second domain and use a domain constraint P^D along (001) to access two 180° domains in the system. In this case, $\vec{P}^D = \frac{1}{2}(\vec{P}_1 - \vec{P}_2)$, so that the constraint on domain polarization corresponds to the constraint of the difference between the polarizations of regions 1 and 2, leading to the formation of two 180° domain walls separating the two domains in periodic boundary conditions. This procedure was used in our previous work[23] on $BaTiO_3$ to study the energetics of domain walls and differs from the constraint on local polarization used by Geneste[35] to study the effect of shape and size of clusters on the free-energy landscape. The evolution of a system from a configuration with uniform polarization (for which P^D is zero) to a domain configuration can provide information about the energetics of the domain wall.

For all constrained-polarization simulations, we start with a zero polarization (or zero P^D) configuration and increase the target polarization (or target P^D) in steps of 2 $\mu C/cm^2$, keeping the temperature fixed. For each value of the target polarization, we thermalize the system with 100 000 time steps and then perform an averaging of various quantities using a run of 100 000 time steps. We use the final configuration of the simulations with the previous target polarization as the initial configuration in the simulation for the next target polarization.

III. RESULTS

A. Ferroelectric transition and hysteresis

First, we perform a heating-up and a cooling-down MD simulation for bulk $PbTiO_3$ using the effective Hamiltonian H_0. The results for the polarization and dielectric constant as a function of temperature are shown in Fig. 1.

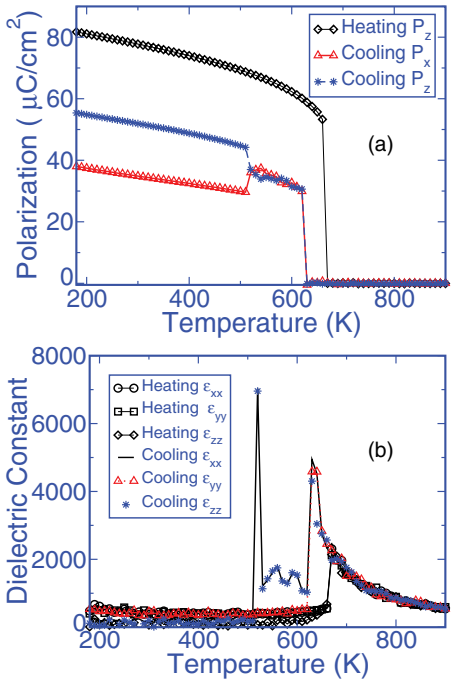

FIG. 1. (Color online) Polarization and dielectric constant as a function of temperature in heating-up and cooling-down molecular-dynamics simulations using the effective Hamiltonian H_0. The P_x and P_y components in the heating-up simulations and the P_y component in the cooling-down simulations are negligible and are not shown in (a) for clarity.

In the heating-up simulation, we started from a low temperature (200 K) with an initial configuration with polarization along the z direction. We increased temperature in steps of 10 K. It can be seen in Fig. 1(a) that the system undergoes a transition from a polar ferroelectric state to a nonpolar paraelectric state at $T = 670$ K. This transition temperature is the same as that found in a previous Monte Carlo study with the same first-principles effective Hamiltonian.[17] In the cooling-down simulation, the transition temperature is about 50 K lower. This hysteresis is typical of a first-order phase transition. It is intriguing that in the cooling-down simulation the system does not transform below the transition to the tetragonal phase with polarization along [001] but to a phase with polarization approximately along [101]. This will be discussed in more detail below.

In the heating-up simulation, the dielectric constant [see Fig. 1(b)] shows a jump at the transition temperature and a peak at the transition in the paraelectric phase, as expected in the soft-mode theory of ferroelectricity. In the cooling-down simulation, the dielectric constant in the paraelectric phase above 670 K is the same as in the heating-up simulation. It then increases smoothly down to 620 K, consistent with metastability of the paraelectric phase in the hysteretic range, but then has a large and variable value down to 500 K. This latter observation is connected to the unexpected [110] direction of the polarization mentioned above and will be discussed in more detail below.

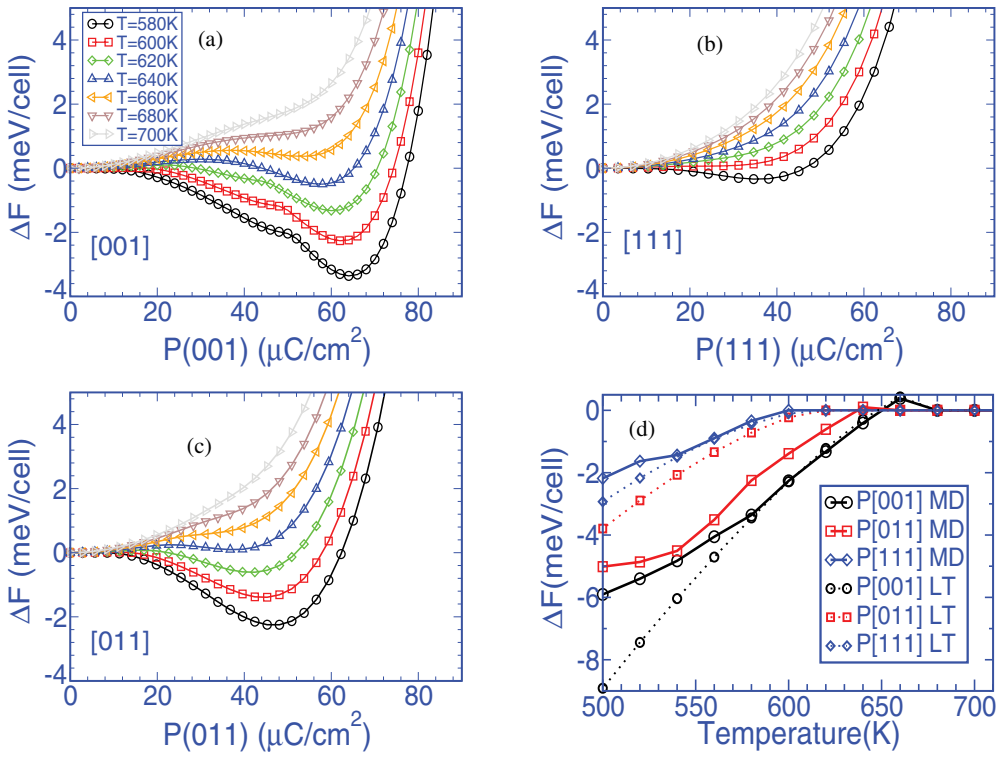

FIG. 2. (Color online) Free-energy differences per unit cell with respect to zero polarization ($P = 0$) as a function of polarization along the (a) [001], (b) [111], and (c) [011] directions for a range of temperatures close to T_c. (d) A comparison of the minimum of the free-energy difference per unit cell [$\Delta F(T) = F(P = P_s) - F(P = 0)$] as a function of temperature along the [001], [011], and [111] directions of polarization from constrained MD simulation and the fitted Landau free-energy function (shown as LT).

B. Free energy of the ferroelectric phase transition

The computed free energies for P along [001], [111], and [011] for a range of temperatures above and below T_c are shown in Figs. 2(a)–2(c). Below T_c, the $\Delta F(P)$ curves for P along [001] show a visible cusp. The reason for this is that for P constrained to values smaller than at the cusp, the system achieves the target polarization by breaking into 90° domains, which we confirmed by examination of configurations in the simulation. Above this value, the curves are well described by the Landau form.

The Landau free-energy functional is very helpful in understanding the behavior of ferroelectrics near the Curie temperature. Here, we write

$$\Delta F(\vec{P},T) = F(0) + A(T - T_c)\left(P_x^2 + P_y^2 + P_z^2\right) + B_1\left(P_x^4 + P_y^4 + P_z^4\right) + B_2\left(P_x^2P_y^2 + P_y^2P_z^2 + P_z^2P_x^2\right) + C\left(P_x^2 + P_y^2 + P_z^2\right)^3 \quad (5)$$

In this simple form of the functional, strain is integrated out, and its effects are absorbed in the values of the coefficients. Thus its applicability is limited to configurations in which the strain is slowly varying in space; for example, we use it below to estimate the contribution to the free energy of domain walls separating domains with essentially uniform polarization.

We determined the parameters for $PbTiO_3$ by fitting to first-principles results for the free energy as a function of $\vec{P}$, obtained by thermodynamic integration for the constrained-polarization molecular-dynamics simulations as explained in Sec. II C. Specifically, we use values of the free energy with P along [001] and [111] for a range of temperatures above T_c, and we do not include the free-energy data below T_c to extract the parameters because constraining polarization to a value smaller than the spontaneous polarization below T_c results in configurations with domains or nonuniform order.[22,25] This yields the parameters given in Table II.

As a measure of how well the functional predicts the behavior near the transition, we found the magnitude of polarization P_s that minimizes the first-principles free energy for each of the three directions of polarization at each temperature. In Fig. 2(d), we show the corresponding free-energy difference [$\Delta F(T) = F(P = P_s) - F(P = 0)$] as a function of temperature for all three directions of polarization, compared with the value of the free-energy difference evaluated with the Landau functional [Eq. (5)]. For P along [001] and [111], the Landau functional is seen to give a good description close to T_c, as

TABLE II. The free-energy parameters of Eq. (5) obtained from fitting MD simulation data above T_c. The values of free energy and polarization used in the fit are in meV and $\mu C/cm^2$, respectively.

Parameter	Value
A	1.48×10^{-5}
T_c (K)	605
B_1	-6.18×10^{-7}
B_2	1.19×10^{-7}
C	8.92×10^{-11}

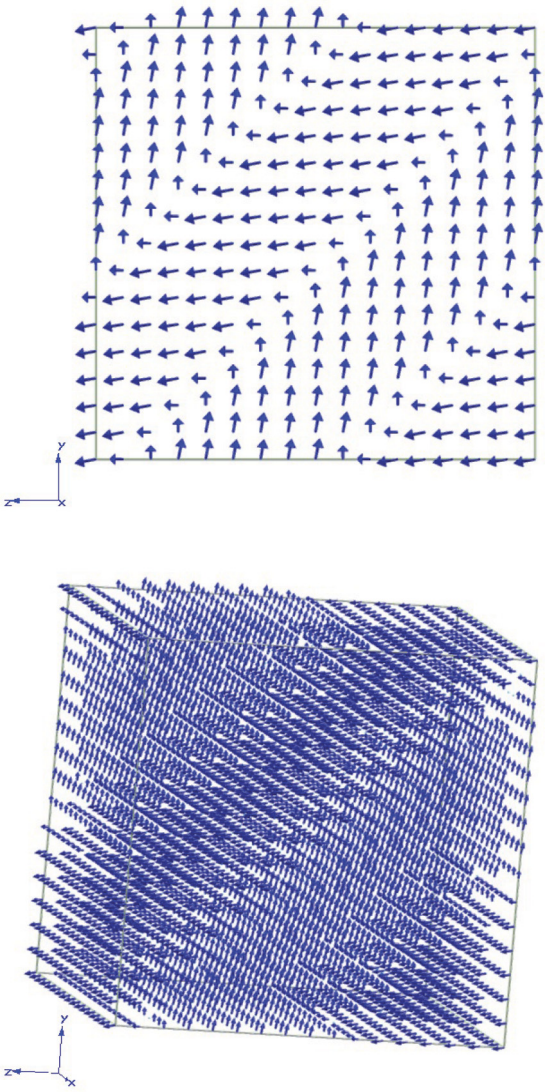

FIG. 3. (Color online) A snapshot of the local dipole moments during constrained MD simulations (constrained P is along [011]) at $T = 520$ K.

expected, with the tetragonal phase being most stable below the first-order transition temperature of 640 K. This value is consistent with the transition temperatures observed on heating and cooling discussed above.

However, the Landau functional completely fails to describe the results for P along [011]. Instead, the minimum free energy for P along [011] is very close to that of the tetragonal phase [see Fig. 2(c)]. We note that a macroscopic polarization along [011] can be obtained either from a homogeneous phase in which all dipoles are aligned along [011] or from a 90° domain phase in which the polarizations of domains are aligned along [001] and [010]. In fact, careful analysis of the configurations in our MD simulations reveals that constraining polarization along [011] leads to the formation of a 90° domain structure (see Fig. 3), with alternate domains of the tetragonal phase with polarization along [001] and [010] directions. This accounts for the fact that the free energy of the 90° domain phase is close to that of the homogeneous tetragonal phase. Also, this is the reason that a 90° domain phase is

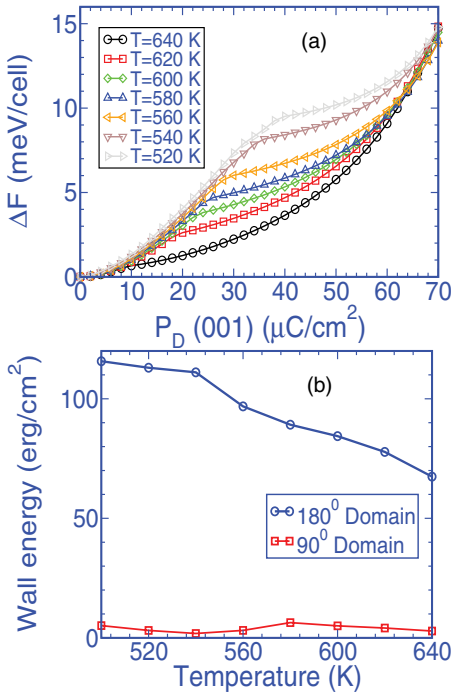

FIG. 4. (Color online) (a) Free-energy differences of domain configurations with respect to uniformly polarized configuration for a range of temperatures and (b) the free energy of the 180° and 90° domain walls as a function of temperature of $PbTiO_3$.

obtained in the unconstrained cooling-down simulation shown in Fig. 1(a). We would like to emphasize that the dielectric constant estimated from the cooling-down simulations provides us the dielectric signature of the 90° domain structure, with a relatively large (∼500) response along the direction perpendicular to the plane of polarization in adjacent domains.

C. Free energy of states with domains

Using the generalized form of the augmented Hamiltonian [Eq. (4)], we obtained the free energy of a 180° domain structure as a function of domain polarization $\vec{P^D} = (0,0,P^D)$ at various temperatures [see Fig. 4(a)]. For a given temperature below T_c, we started from a uniformly polarized state and increased P^D in steps of 2 μC/cm^2. For small P^D, the polarizations in the two regions are aligned with magnitude modulated by P^D. At a critical value of P^D that increases with decreasing temperature, 180° domains form. At this value, the nuclei with opposite polarization that form in the simulations exceed critical size. The initial increase in free energy until the state changes from uniform polarization to the one with domains is the free-energy barrier associated with the formation of a nucleus of critical size. With a further increase in P^D, the free energy remains essentially constant (the nearly flat part of the free-energy curve) up to $P^D = P_s$, the spontaneous polarization at that temperature, and then increases for higher values of P^D. The absence of local minima for P^D larger than the critical value is due to the fact that the system size considered here is too small to stabilize two 180° domains. We find that two 180° domains can be easily stabilized in a larger system size of $40 \times 16 \times 16$ unit cells.

The 180° domain-wall energy at a temperature is obtained from $\gamma_D(T) = \Delta F(P^D = P_s)/(2L_yL_z)$, where P_s is the spontaneous polarization of the system at that temperature. The factor of 2 is due to the fact that two domain walls are present in our systems under periodic boundary conditions. Our estimate of the domain-wall energy as a function of temperature (see Fig. 4) is comparable to earlier estimates.[36,37] The 180° domain-wall energy for $PbTiO_3$ is about 15 times larger than that of $BaTiO_3$.[23] This large difference is expected due to the fact that strain-polarization coupling is larger in $PbTiO_3$ than in $BaTiO_3$.

To estimate the 90° domain-wall free energy, we take the free energy from the MD simulation with constrained polarization along [011] and subtract the free energy for the simulation with polarization along [001] [see Fig. 2(c)]. We find that the 90° domain-wall energy in $PbTiO_3$ is much smaller than the 180° domain-wall energy, indicating that the system can easily form 90° domains. This is consistent with the recent experimental observation of 90° domains in $PbTiO_3$.[38]

D. Dielectric response of domain configurations

The dielectric response of a system having 180° domains is shown in Fig. 5, with the dielectric response of a system with uniform polarization (obtained from the heating-up simulation previously shown in Fig. 1) included for comparison. In the 180° domain simulation, at each temperature the system is constrained to a domain polarization, $P^D = 66\ \mu C/cm^2\ \hat{z}$ (which is the spontaneous polarization at temperature $T = 580$ K). The high-temperature behavior, above T_c, of all three components of the dielectric response of the system with 180° domains is weak. This difference in the dielectric response of the system with 180° domains and the system with uniform polarization above T_c is expected because constraining $P^D = 66\ \mu C/cm^2$ for domain configurations strongly suppresses fluctuations, whereas the system with uniform polarization fluctuates around zero polarization. Below T_c, the dielectric response of the 180° domain configurations along the direction of P (i.e., zz component) is rather weak, comparable to that of the uniformly polarized state below 600 K (see Fig. 5). The dielectric response along the direction perpendicular to polarization and in the plane of the domain wall (i.e., yy component) is enhanced relative to uniform polarization and comparable to that of the 90° domain structure.

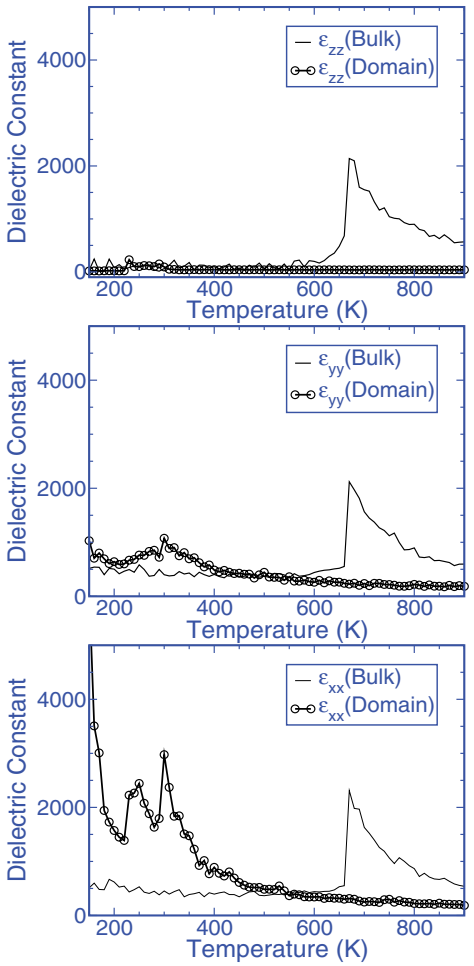

FIG. 5. (Color online) Dielectric constant of 180° domain configurations compared to a uniformly polarized configuration (shown as bulk) of $PbTiO_3$ as a function of temperature.

In contrast, at low temperatures the response along the direction perpendicular to the plane of the domain wall (i.e., xx component) is anomalously high. This behavior can be attributed to the constraint on P^D. As the temperature is decreased, the spontaneous polarization in the two domains becomes larger than the constrained domain polarization at a point close to the temperature at which the dielectric response starts to increase. To satisfy the constraint, the domain wall fluctuates, resulting in sites where the local polarization is opposite to $\hat{e}$ of Eq. (4); this also results in a nonzero polarization for the system, consistent with simulation results (not shown). In the vicinity of steps in the domain wall, the other components of the local polarization can take on nonzero values. The constraint can also be satisfied by reducing the z component of the local polarization near the wall, which would tend to favor an increase in the other components and correspondingly an increase in the fluctuation of their values. The fact that these effects are so much stronger in the direction perpendicular to the wall, especially at very low temperatures, is quite striking and suggests further investigation.

Our finding of large dielectric responses for inhomogeneously ordered states thus is seen to arise from the imposition of a constraint that is inconsistent with the most favorable state and leads to a multiplicity of states with a distribution in polarization. While the constraint we have imposed here would be difficult to realize in an experimental system, this suggests a potentially promising design principle for systems with a large dielectric response.

IV. SUMMARY AND CONCLUSIONS

Using a first-principles effective Hamiltonian in constrained-polarization molecular-dynamics simulations, we determined the free-energy landscape for $PbTiO_3$ near its ferroelectric phase transition. A comparison of the free energies of states with polarization along different directions shows that the tetragonal phase is thermodynamically stable for all temperatures below the ferroelectric transition temperature. For some temperature range close to 520 K an *orthorhombic-like* metastable phase becomes

very close in energy to the tetragonal phase. However, a close examination of this phase reveals a 90° domain structure.

We also used a generalized form of the effective Hamiltonian to study the energetics of configurations consisting of ferroelectric domains, determining the domain-wall energies of 90° and 180° domain walls as a function of temperature, the former being an order of magnitude lower in energy than the latter. As a prediction to aid the interpretation of experiments, we show that the dielectric response of $PbTiO_3$ bears interesting signatures of the domain structure and that it is anomalously larger than that of the uniformly polarized state. Our finding provides a possible explanation for why observed dielectric response of ferroelectrics is often significantly larger than the one estimated from first-principles calculations of phonons.

ACKNOWLEDGMENTS

A.K. gratefully acknowledges the Council of Scientific and Industrial Research (CSIR), India, for the research support and the Centre for Computational Material Science (CCMS), JNCASR, for providing computational facilities. U.V.W. acknowledges funding from an IBM Faculty award and a DAE outstanding researcher fellowship. We thank David Vanderbilt for stimulating discussions.

[1] M. E. Lines and A. M. Glass, *Principles and Applications of Ferroelectrics and Related Materials* (Oxford University Press, New York, 1977).
[2] J. F. Scott, Science **315**, 954 (2007).
[3] M. Dawber, P. Chandra, P. B. Littlewood, and J. F. Scott, J. Phys. Condens. Matter **15**, L393 (2003).
[4] K. Rabe, Ch. H. Ahn, and J.-M. Triscon, *Physics of Ferroelectrics: A Modern Perspective* (Springer, Berlin, 2007).
[5] D. Vanderbilt, Current Opinion in Solid State and Materials Science **2**, 701 (1997).
[6] J. J. Wang, P. P. Wu, X. Q. Ma, and L. Q. Chen, J. Appl. Phys. **108**, 114105 (2010).
[7] Y. L. Li, L. E. Cross, and L. Q. Chen, J. Appl. Phys. **98**, 064101 (2005).
[8] G. Akcay, J. V. Mantese, G. A. Rossetti, and S. P. Alpay, Appl. Phys. Lett. **90**, 242909 (2007).
[9] S. Zhong, V. Nagarajan, and S. P. Alpay, J. Mater. Res. **21**, 1600 (2006).
[10] S. C. Hwang, J. E. Huber, R. M. McMeeking, and N. A. Fleck, J. Appl. Phys. **84**, 1530 (1998).
[11] E. B. Tadmor, U. V. Waghmare, G. S. Smith, and E. Kaxiras, Acta Mater. **50**, 2989 (2002).
[12] R. E. Cohen, Nature (London) **358**, 136 (1992).
[13] R. D. King-Smith and D. Vanderbilt, Phys. Rev. B **49**, 5828 (1994).
[14] K. M. Rabe and J. D. Joannopoulos, Phys. Rev. Lett. **59**, 570 (1987).
[15] W. Zhong, D. Vanderbilt, and K. M. Rabe, Phys. Rev. Lett. **73**, 1861 (1994).
[16] W. Zhong, D. Vanderbilt, and K. M. Rabe, Phys. Rev. B **52**, 6301 (1995).
[17] U. V. Waghmare and K. M. Rabe, Phys. Rev. B **55**, 6161 (1997).
[18] T. Nishimatsu, M. Iwamoto, Y. Kawazoe, and U. V. Waghmare, Phys. Rev. B **82**, 134106 (2010).
[19] D. Vanderbilt and M. H. Cohen, Phys. Rev. B **63**, 094108 (2001).
[20] A. J. Bell, J. Appl. Phys. **89**, 3907 (2001).
[21] A. P. Giddy, M. T. Dove, and V. Heine, J. Phys. Condens. Matter **1**, 8327 (1989).
[22] A. Troster, C. Dellago, and W. Schranz, Phys. Rev. B **72**, 094103 (2005).
[23] A. Kumar and U. V. Waghmare, Phys. Rev. B **82**, 054117 (2010).
[24] G. Geneste, Phys. Rev. B **79**, 064101 (2009).
[25] G. Geneste, Comput. Phys. Commun. **181**, 732 (2010).
[26] T. Nishimatsu, U. V. Waghmare, Y. Kawazoe, and D. Vanderbilt, Phys. Rev. B **78**, 104104 (2008).
[27] FERAM, http://loto.sourceforge.net/feram.
[28] J. Paul, T. Nishimatsu, Y. Kawazoe, and U. V. Waghmare, Phys. Rev. Lett. **99**, 077601 (2007).
[29] U. V. Waghmare, E. J. Cockayne, and B. P. Burton, Ferroelectrics **291**, 187 (2003).
[30] B. P. Burton, E. Cockayne, and U. V. Waghmare, Phys. Rev. B **72**, 064113 (2005).
[31] S. D. Bond, B. J. Leimkuhler, and B. B. Laird, J. Comput. Phys. **151**, 114 (1999).
[32] K. M. Rabe and U. V. Waghmare, Phys. Rev. B **52**, 13236 (1995).
[33] D. Frenkel and B. Smith, *Understanding Molecular Simulation: From Applications to Algorithm* (Academic, San Diego, CA, 2002).
[34] A. Troster and K. Binder, J. Phys. Condens. Matter **24**, 284107 (2012).
[35] G. Geneste, J. Phys. Condens. Matter **23**, 125901 (2011).
[36] S. Poykko and D. J. Chadi, Appl. Phys. Lett. **75**, 2830 (1999).
[37] W. J. Merz, Phys. Rev. **95**, 690 (1954).
[38] T. Nishimatsu, K. Aoyagi, T. Kiguchi, T. J. Konno, Y. Kawazoe, H. Funakubo, A. Kumar, and U. V. Waghmare, J. Phys. Soc. Jpn. **81**, 124702 (2012).